On the statistical behavior of planar velocity parameters in crossed-path and multi-path arrangements using ATT method

J. Lanzersdorfer
Andritz AG, Graz, Austria
johannes.lanzersdorfer@andritz.com

July 24, 2014

Abstract

The acoustic transit time (ATT) method is commonly used to measure volume flow rates of liquid and gaseous media. We therefore determine axial planar mean velocities at certain elevations within a measuring section and integrate them over the corresponding wetted cross-section of the conduit. I provide evidence that the commonly used acoustic arrangement with symmetric crossed paths represents a very special case of a general multi-path setup. This new approach is confronted with the widely used ray tracing approximation. It gives rise to statistical uncertainties of the planar velocity parameters which have not been taken into account so far by any standard test code. Furthermore, it offers new innovative possibilities like close-by arrangements which seem to produce more reliable results in sections with local flow anomalies.

1 Introduction

Several international or national test codes accepts already the acoustic transit-time method (ATT) as a method for absolute flow measurement, for instance [1, 2]. We expect the integration of this measurement technique into the main part of the test code IEC 60041 in the upcoming revision within the next few years. That is, we will face a high boost of temporary or stationary ATT installations on site for hydraulic efficiency testing.

ATT systems feature high precision in repeatability and reproducibility and thus represent a powerful device with very low measurement uncertainty after in-situ calibration. Good repeatability and reproducibility are desirable properties for a flow metering device but they do not lead to low uncertainties for non-calibrated installations consequently. It has often been stated in literature but it is worth repeating it: the terms *precision* and *uncertainty* do not mean the same [3]. The community of hydraulic engineering has gained great practical experience since 1991, when the last revision of the IEC 60041 test code was issued [4]. We notice refinements in theory especially in using flow integration procedures, which are closer to physical reality [5, 6], and in accounting for sensor protrusion [7]. Pairs of axisymmetric, crossed chordal paths have established to be the standard to diminish the negative impact of cross flow. However, the application of crossed paths demonstrates only a special case of two paths in an axially parallel acoustic plane. A recently published article uses a statistical approach to determine the propagation velocity of an acoustic pulse between sensor pairs [8]. It reveals:

1. A number of $n \geq 2$ paths per axially parallel plane is required to obtain a statistical quantification of contributing planar velocity parameters c_i, $v_{\|,i}$ and $v_{\perp,i}$ denoting the mean values at plane i of the speed of sound, the axial velocity and the transveral velocity, respectively.

2. We cannot access the impact of any cross flow if we use only a single acoustic path per plane. This type of arrangement should therefore never be used for guarantee verifications.

3. We conclude from point 1 that the statistical approach assigns random uncertainties to the planar velocities which have not yet been taken into account when estimating the uncertainty of the flow rate.

4. The alternative approach reproduces the velocity formula for crossed paths, which is commonly used.

5. When using an axisymmetric crossed path arrangement; the inclination angle $\varphi = \pi/4$ exhibits the lowest random uncertainty.

6. Furthermore, we deduce from point 1 that the 2-path or the multi-path ensemble in *close-by* arrangement can be favorable in presence of asymmetric flow profiles.

With this paper I want to give a more detailed look in comparing the standard crossed path arrangement with the proposed close-by arrangement from a statistical point of view. So, we can gain information of the individual strengths and weaks.

2 Theoretical background

2.1 Ray tracing approach

The usual planar velocity equations given in various test codes are based on a ray tracing approximation [9]. It should be noted that such an approximation is only valid if the wave length of the propagating acoustic pulse is small compared to the beam width and the beam width is small compared to the pipe dimensions [10]. Both criteria are usually satisfied for testing large-scale hydraulic machines. Here, I give a survey in the derivation of the velocity equations in using two (2) paths arbitrarily aligned within the same acoustic plane. At the end, we will see that the determination of the axial velocity with the metrological instrumentation commonly in use is only accessible with several simplifications of our physical system.
Figures 1(a) and 1(b) illustrate the definition of the main geometric parameters. Here, we focus figure 1(b) for the subsequent derivation of the velocity equations in using two (2) paths arbitrarily aligned within the same acoustic plane. The origin of our two-dimensional Carthesian coordinate system $(0|0)$ is equal to the location of sensor 1 on the left conduit wall, the positive directions of x and y-coordinates are defined from bottom to the top and from left to the right, respectively. The positive direction of axial flow and transverse flow are defined analogously. Let us start in considering the physical conditions of a sensor pair forming path no. 1. An acoustic pulse is emitted from the sensor on the left under an central angle of φ_{1L}, which is generally not ident with φ_{11}, and detected by the sensor on the right.

Simplification I The flow of the fluid is stationary.

Simplification II The acoustic pluse propagates only on the x-y-plane.

Simplification III The speed of sound c remains constant along the acoustic path.

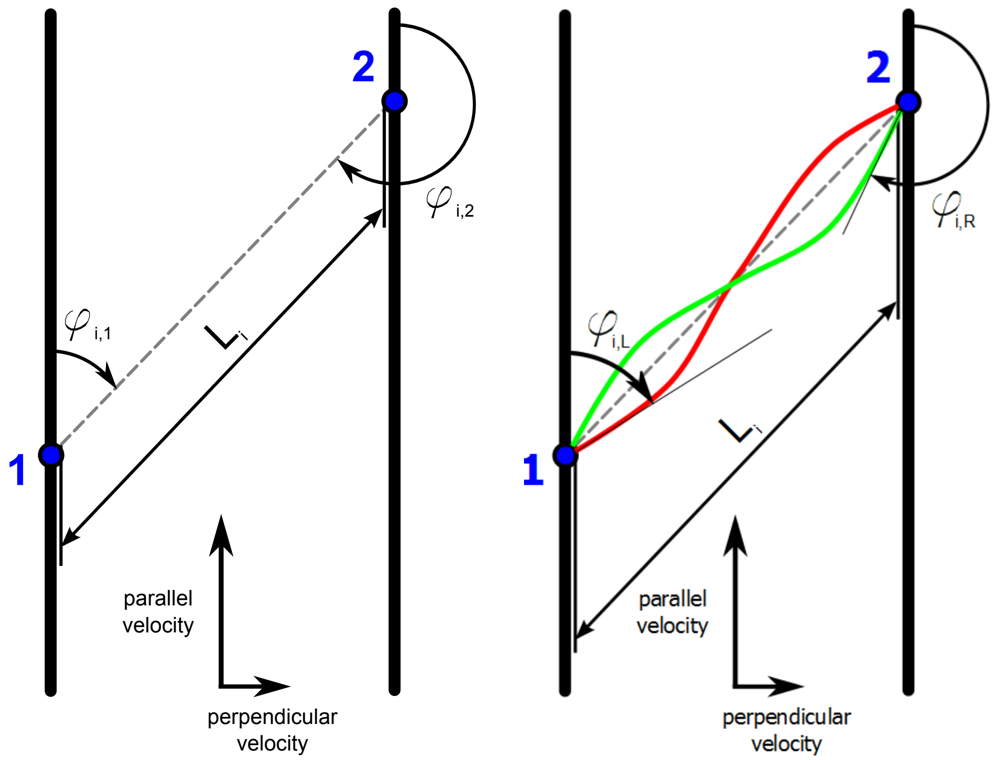

(a) Theoretically ideal acoustic path (gray dashed line), parallel velocity $v_\parallel$, perpendicular velocity $v_\perp$, acoustic path length L_i, left path angle φ_{i1} with respect to the conduit axis, right path angle $\varphi_{i,2} = \varphi_{i1} + \pi$ (source: [8]).

(b) Real path geometry projected onto the two-dimensional plane (exaggerated representation): Path of downstream travelling acoustic pulse (red), path of upstream travelling pulse (green), central emitting angles of acoustic power, φ_{iL} and φ_{iR}.

Figure 1: Geometry of an acoustic path no. i inside the conduit

With the simplifications above the velocity at time t of the *downstream travelling* pulse yields

$$\begin{pmatrix} w_x(t) \\ w_y(t) \end{pmatrix} = c \begin{pmatrix} \cos\varphi_{1L} \\ \sin\varphi_{1L} \end{pmatrix} + \begin{pmatrix} v_\parallel(x(t),y(t)) \\ v_\perp(x(t),y(t)) \end{pmatrix} . \tag{1}$$

Integration between zero time and the measured average travelling time $\hat{\tau}_{11}$ gives the position vector

$$L_1 \cdot \begin{pmatrix} \cos\varphi_{11} \\ \sin\varphi_{11} \end{pmatrix} = \hat{\tau}_{11} \cdot c \begin{pmatrix} \cos\varphi_{1L} \\ \sin\varphi_{1L} \end{pmatrix} + \int_0^{\hat{\tau}_{11}} \begin{pmatrix} v_\parallel(x(t),y(t)) \\ v_\perp(x(t),y(t)) \end{pmatrix} dt . \tag{2}$$

Equation (2) reveals the main drawback of the ATT method what makes us going round in circles: A proper calculation of the mean velocity parameters requires the knowledge of the available velocity distribution. We therefore simplify the circumstances with

Simplification IV The averaged flow field is approximated by

$$\begin{pmatrix} v_\parallel \\ v_\perp \end{pmatrix} \approx \frac{1}{\hat{\tau}_{11}} \int_0^{\hat{\tau}_{11}} \begin{pmatrix} v_\parallel(x(t),y(t)) \\ v_\perp(x(t),y(t)) \end{pmatrix} dt$$

which facilitates (2) to

$$L_1 \cdot \begin{pmatrix} \cos\varphi_{11} \\ \sin\varphi_{11} \end{pmatrix} = \hat{\tau}_{11} \cdot \left[c \begin{pmatrix} \cos\varphi_{1L} \\ \sin\varphi_{1L} \end{pmatrix} + \begin{pmatrix} v_\parallel \\ v_\perp \end{pmatrix} \right] . \tag{3}$$

We conclude, from a mathematical point of view, that the four (4) unknown variables in the two (2) equations above represent an under-determined system of nonlinear equations. We require additional information (equations and/or side conditions) to solve our problem. Let us continue to the upstream propagating conditions where a similar approach yields

$$-L_1 \cdot \begin{pmatrix} \cos\varphi_{11} \\ \sin\varphi_{11} \end{pmatrix} = \hat{\tau}_{12} \cdot \left[c \begin{pmatrix} \cos\varphi_{1R} \\ \sin\varphi_{1R} \end{pmatrix} + \begin{pmatrix} v_\parallel \\ v_\perp \end{pmatrix} \right] . \tag{4}$$

The new system of equations is still under-determined (5 unknown variables versus 4 equations). It can be solved exactly only if one unknown parameter can be estimated with appropriate accuracy.[1] However, a proper approach

[1] A usual way is to neglect the transversal flow $v_\perp$ in presence of excellent parallel inflow conditions.

requires an additional sensor pair forming path no. 2. We handle the problem with a generally orientated planar inclination angle $\varphi_{21} \neq \varphi_{11}$, which gives us subsequently two (2) new unknown variables and the following four (4) new equations

$$L_2 \cdot \begin{pmatrix} \cos\varphi_{21} \\ \sin\varphi_{21} \end{pmatrix} = \hat{\tau}_{21} \cdot \left[c \begin{pmatrix} \cos\varphi_{2L} \\ \sin\varphi_{2L} \end{pmatrix} + \begin{pmatrix} v_{\|} \\ v_{\perp} \end{pmatrix} \right] \text{ and} \tag{5}$$

$$-L_2 \cdot \begin{pmatrix} \cos\varphi_{21} \\ \sin\varphi_{21} \end{pmatrix} = \hat{\tau}_{22} \cdot \left[c \begin{pmatrix} \cos\varphi_{2R} \\ \sin\varphi_{2R} \end{pmatrix} + \begin{pmatrix} v_{\|} \\ v_{\perp} \end{pmatrix} \right] . \tag{6}$$

That is, we end up with seven (7) unknowns in eight (8) equations, which represents an over-determined system of nonlinear equations. This system cannot be solved exactly but approximately yielding a not evident but commonly used equation for the axial velocity

$$v_{\|} = \frac{L_1 \sin\varphi_{21} \left(\frac{1}{\hat{\tau}_{11}} - \frac{1}{\hat{\tau}_{12}} \right) - L_2 \sin\varphi_{11} \left(\frac{1}{\hat{\tau}_{21}} - \frac{1}{\hat{\tau}_{22}} \right)}{2 \left(\cos\varphi_{11} \sin\varphi_{21} - \cos\varphi_{21} \sin\varphi_{11} \right)} \tag{7}$$

Remarks

- Equation (7) is the result of several simplifications done during the whole derivation processus and it is an approximation of the mathematically exact solution. A (random) expanded uncertainty $t \cdot u(v_{\|})$ with $df = 8 - 7 = 1$ statistical degrees of freedom has to be assigned to the axial velocity value but has never been treated by any standard test code.
- We could construct an analytically exact solution of the axial velocity (6 unknowns versus 6 equations) in omitting two equations of any path along a distinct acoustic direction, for instance, we put away the equations given in (5). Permuting the set of equations yields consequently $\begin{pmatrix} 4 \\ 3 \end{pmatrix} = 4$ different values of the axial velocity. The mean value of those results may be considered as final parameter estimate with $df = 4 - 1 = 3$, i.e., we obtain again an additional uncertainty of random nature. However, equation (7) generally yields more reliable results since measurement errors do not impact that hard on the calculation procedure. In fact, I have never seen any testing using such an approach.

2.2 Statistical approach

The theoretical approach described in reference [8] uses the approximation of the propagation velocity of an acoustic pulse emitted by sensor j which travels along the theoretical path i to the opposite sensor

$$\frac{L_i}{\hat{\tau}_{ij}} \approx c + \cos\varphi_{ij} \cdot v_{\parallel} + \sin\varphi_{ij} \cdot v_{\perp} \tag{8}$$

The parameters L_i and $\hat{\tau}_{ij}$ denote the planar distance between the relevant sensor pair and the mean propagation time between these sensors. The inclination angle φ_{ij} is defined in accordance with figure 1(a). For each path in the same acoustic plane we obtain two equations when using forward and backward propagation between the pair of sensors. An equiweighted linear regression yields for the axial velocity

$$v_{\parallel} = \frac{1}{N} \cdot \left[\overline{\left(\frac{L \cdot \cos\varphi}{\hat{\tau}}\right)} \cdot \overline{\sin^2\varphi} - \overline{\left(\frac{L \cdot \sin\varphi}{\hat{\tau}}\right)} \cdot \overline{\cos\varphi \sin\varphi} \right] \tag{9}$$

with

$$N = \overline{\cos^2\varphi} \cdot \overline{\sin^2\varphi} - \overline{\cos\varphi \sin\varphi}^2 . \tag{10}$$

In this paper, the average value of any function $f(x)$ is denoted by $\overline{f(x)}$ which is the arithmetic mean over the two indices i and j

$$\overline{f(x)} = \frac{1}{2n} \sum_{i=1}^{n} \sum_{j=1}^{2} f(x_{ij}) \tag{11}$$

However, the standard uncertainty of the axial velocity gives

$$u(v_{\parallel}) = s \cdot \sqrt{\frac{\overline{\sin^2\varphi}}{2nN}} \tag{12}$$

with the standard uncertainty of the measured propagation velocity with respect to the regression model function, s, obtained from

$$s^2 = \frac{2n}{2n-m} \left\{ \overline{\left(\frac{L}{\hat{\tau}}\right)^2} - \overline{\left(\frac{L}{\hat{\tau}}\right)}^2 - \frac{1}{N} \left[\overline{\left(\frac{L \cdot \cos\varphi}{\hat{\tau}}\right)}^2 \cdot \overline{\sin^2\varphi} + \overline{\left(\frac{L \cdot \sin\varphi}{\hat{\tau}}\right)}^2 \cdot \overline{\cos^2\varphi} - 2\overline{\left(\frac{L \cdot \cos\varphi}{\hat{\tau}}\right)} \cdot \overline{\left(\frac{L \cdot \sin\varphi}{\hat{\tau}}\right)} \cdot \overline{\cos\varphi \sin\varphi} \right] \right\} . \tag{13}$$

We denote the number of paths in the same acoustic plane by n, the number of regressors $m = 3$.

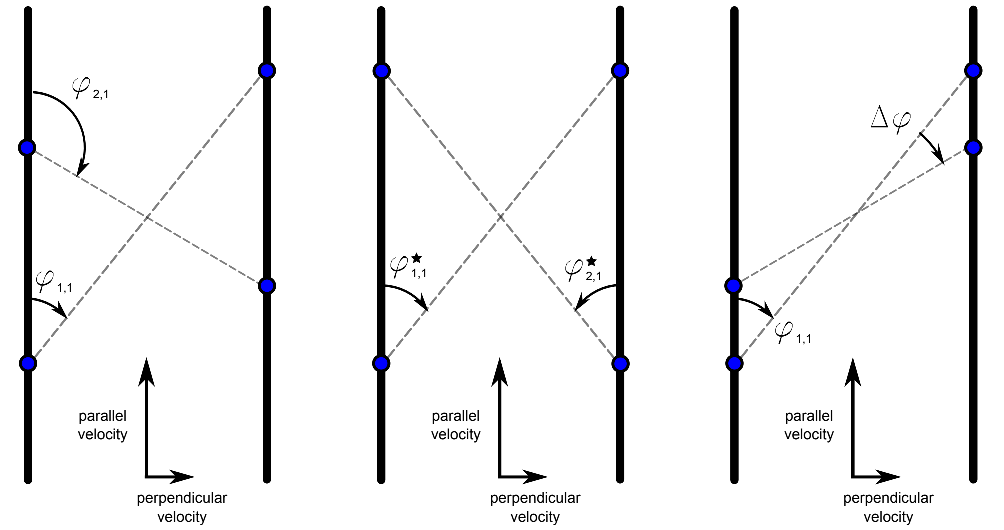

(a) General arrangement (b) Symmetric arrangement (c) Close-by arrangement

Figure 2: Geometry of arrangements with two planar paths (source: [8])

2.2.1 Two-path arrangement

We obtain for two paths per plane, i.e., $n = 2$, in the general case (view figure 2(a))

$$v_\parallel = \frac{L_1 \sin\varphi_{21}\left(\frac{1}{\hat{\tau}_{11}} - \frac{1}{\hat{\tau}_{12}}\right) - L_2 \sin\varphi_{11}\left(\frac{1}{\hat{\tau}_{21}} - \frac{1}{\hat{\tau}_{22}}\right)}{2\left(\cos\varphi_{11}\sin\varphi_{21} - \cos\varphi_{21}\sin\varphi_{11}\right)} \tag{14}$$

and

$$u(v_\parallel) = \frac{\sqrt{\sin^2\varphi_{11} + \sin^2\varphi_{21}}}{2\sqrt{2}|\cos\varphi_{11}\sin\varphi_{21} - \cos\varphi_{21}\sin\varphi_{11}|} \cdot \left| L_1\left(\frac{1}{\hat{\tau}_{11}} + \frac{1}{\hat{\tau}_{12}}\right) - L_2\left(\frac{1}{\hat{\tau}_{21}} + \frac{1}{\hat{\tau}_{22}}\right)\right| , \tag{15}$$

The symmetric case (figure 2(b)) simplifies the equations above. The inclination angle of the second path yields $\varphi_{21} = \pi - \varphi_{11}$, and the axial velocity is

$$v_\parallel = \frac{L_1\left(\frac{1}{\hat{\tau}_{11}} - \frac{1}{\hat{\tau}_{12}}\right) - L_2\left(\frac{1}{\hat{\tau}_{21}} - \frac{1}{\hat{\tau}_{22}}\right)}{4\cos\varphi_{11}} \tag{16}$$

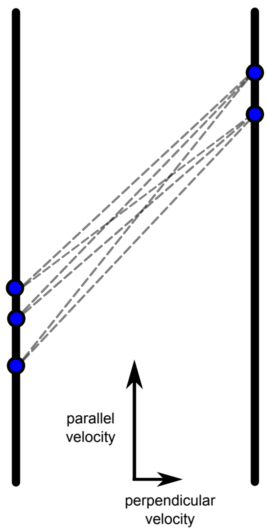

Figure 3: Geometry of multiple acoustic paths in close-by arrangement: This example shows $n_1 = 3$ sensors on the left and $n_2 = 2$ sensors on the right spanning an acoustic plane with $n = 6$ paths (source: [8]).

and the corresponding standard uncertainty

$$u(v_\parallel) = \frac{\left| L_1 \left(\frac{1}{\hat{\tau}_{11}} + \frac{1}{\hat{\tau}_{12}} \right) - L_2 \left(\frac{1}{\hat{\tau}_{21}} + \frac{1}{\hat{\tau}_{22}} \right) \right|}{4 |\cos \varphi_{11}|} , \tag{17}$$

Finally, when applying *close-by* arrangements, where ($\varphi_{21} = \varphi_{11} + \Delta\varphi$) with $|\Delta\varphi| \ll \pi/2$, we obtain

$$v_\parallel = \frac{1}{2 \sin \Delta\varphi} \left[L_1 \sin(\varphi_{11} + \Delta\varphi) \left(\frac{1}{\hat{\tau}_{11}} - \frac{1}{\hat{\tau}_{12}} \right) - L_2 \sin \varphi_{11} \left(\frac{1}{\hat{\tau}_{21}} - \frac{1}{\hat{\tau}_{22}} \right) \right] \tag{18}$$

and

$$u(v_\parallel) = \sqrt{\frac{\sin^2 \varphi_{11} + \sin^2(\varphi_{11} + \Delta\varphi)}{8 \sin^2 \Delta\varphi}} \cdot \left| L_1 \left(\frac{1}{\hat{\tau}_{11}} + \frac{1}{\hat{\tau}_{12}} \right) - L_2 \left(\frac{1}{\hat{\tau}_{21}} + \frac{1}{\hat{\tau}_{22}} \right) \right| . \tag{19}$$

2.2.2 Multi-path arrangement

Reference [8] reveals that under constant measurement conditions, the expanded uncertainty, $t \cdot u(v_\parallel)$, diminishes only with a higher number of paths

n, which reduces the standard deviation $u(v_\parallel) \propto 1/\sqrt{n}$ and also the Student's t-value ($df = 2n - m$). Therefore, using more than two planar paths is recommended whenever test code requirements in terms of flow conditions and geometry are not met.

The fact that sensors emit the main portion of the acoustic energy in a cone opens up an interesting way of using multiple paths in a close-by arrangement. Sensors can be positioned on opposite conduit walls as depicted in figure 3. Then, each detector on the right is able to receive non-reflected signals from all emitters on the left and vice versa. That is, all sensors on one wall are within the visual field of the sensors on the opposite wall. With n_1 as the number of sensors on the left and n_2 as the number of sensors on the right, the total number of acoustic paths is

$$n = n_1 \cdot n_2 \tag{20}$$

3 Discussion

In the following subsections we consider a homogeneous fluid under global stationary flow conditions confined by parallel conduit walls. There we discuss the advantages and drawbacks of the individual path arrangements. We assume an axial velocity distribution, which does not alter within the acoustic measurement section.

3.1 A word on the stationarity of flow

The examination of a stationary flow has been the first simplification in deriving the ray tracing approximation in section 2.1. It also represents the crucial criterion for the measurement quality using the statistical approach. Imagine an time variant flow behavior, then it makes no big difference which path arrangement is used since the individual paths and path directions can only to be sampled successively using state-of-the-art technology.

3.2 Negligible cross flow conditions and negligible local flow anomalies

It is a given that under such hydraulically favorable conditions the symmetrical arrangement with crossed paths under $\varphi^\star = \pi/4$ exhibits the best vector resolution and thus the lowest random uncertainty. I do not expect any other double-path arrangement to deliver more accurate measurement results.

3.3 Constant cross flow conditions and negligible local flow anomalies

If the transveral flow drift could be considered as globally constant (within the measurement section) the symmetrical, crossed paths are to favor in contrast to the close-by arrangement. Since we desist from any impact of locally existing flow phenomena, both paths face equal ratios of $v_{\parallel}(x,y)/v_{\perp}(x,y) = v_{\parallel}(y)/v_{\perp}(y)$ independent of the x-coordinate. Nevertheless, constant planar cross flow conditions are atypical and seldom.

3.4 Negligible cross flow conditions and non-negligible local flow anomalies

It may happen that the local flow behavior changes significantly in the wake of a sensor. The signal from or to another downstream mounted sensor can hence be affected. However, such an effect seems to impact the measurements only at high dimensional ratios (sensor size)/(conduit width). Symmetric crossed paths are to favor.

3.5 General cross flow conditions with or without local flow anomalies

These flow conditions represent by far the most frequent case since design engineering and metrological engineering do not harmonize per definition. As a consequence of this, if we strictly obeyed the recommendations of the test codes (i.e., straight and uniform length $> 10D$ upstream and $> 3D$ downstream the measurement section [4]), hardly any measurements could be done in accordance with the code. Despite of a non-changing axial velocity distribution the ratio $v_{\parallel}(x,y)/v_{\perp}(x,y)$ clearly shows a dependency on the x-coordinate. That is, the larger the angular offset between both paths – as typical for symmetrical crossed paths – the bigger the negative impact of the non-axial flow conditions on the measurement quality. The application of a close-by arrangement reveals here advantages when considering here the flow ratio $v_{\parallel}(x,y)/v_{\perp}(x,y)$. We may assume that both paths face almost identical flow conditions, i.e., $v_{\parallel}(x,y)/v_{\perp}(x,y) \approx v_{\parallel}(y)/v_{\perp}(y)$ as under the constant cross flow conditions. Despite of the poorer vectorial resolution reliable measurements can be expected with close-by paths even under unfavorable flow conditions. If higher resolution and low random uncertainty are required a multipath arrangement as described in section 2.2.2 will be the right choice. The path limitations are normally set by financial aspects in using a higher number of sensors and additional installation time.

4 Conclusion

The determination of the planar axial velocity using two different approaches have been compared with (i.e., ray tracing approximation versus statistical approach). Both procedures yield identical equations for general two-path arrangement and give rise to an additional random uncertainty, which finally impacts the uncertainty estimation of the volume flow rate. I propose the implementation of this contributing uncertainty proportion into the upcoming revisions of relevant international standard test codes as it is IEC 60041. The behavior of symmetrical crossed path arrangements and close-by/multipath arrangements have been discussed showing clear advantages of the latter under stationary but non-favorable flow conditions.

Nomenclature

Symbol	Description	Unit
c	Speed of sound	(m/s)
D	Characteristic conduit width	m
df	Statistical degrees of freedom	(-)
L_i	Minimum distance between both sensors of path i	(m)
m	Number of regressors (= 3)	(-)
n	Number of paths in the same plane	(-)
s	Standard uncertainty of the measured propagation velocities with respect to the linear regression model function	(m/s)
t	Time	(s)
u	Standard uncertainty	(a.u.)
$v_{\parallel}$	Mean axial velocity	(m/s)
$v_{\perp}$	Mean transversal velocity	(m/s)
w	Velocity of the acoustic pulse	(m/s)
$\hat{\tau}_{ij}$	Mean transit time of acoustic pulse along path i emitted from sensor j based on m observations ($= \sum_{k=1}^{m} \tau_{i,j}(k)/m$)	(s)
φ_{ij}	Inclination angle of path i with respect to the conduit wall of sensor j (clockwise rotation)	(rad)

References

[1] ISO, editor. *ISO 6416 – Hydrometry – Measurement of discharge by the ultrasonic (acoustic) method.* ISO, 2004.

[2] ASME, editor. *ASME PTC 18 – Hydraulic turbines and pump-turbines performance test codes.* ASME, 2011.

[3] JCGM, editor. *JCGM 100 – Evaluation of measurement data – Guide to the expression of uncertainty in measurement. JCGM 100:2008. GUM 1995 with minor corrections.* BIPM, 1 edition, 2008.

[4] IEC, editor. *IEC 60041 – Field acceptance tests to determine the hydraulic performance of hydraulic turbines, storage pumps and pump-turbines.* IEC, 3 edition, 1991.

[5] T. Staubli, A. Voser, J.-E. Prénat, and C. Bruttin. The Swiss National Energy Foundation Project on Acoustic Discharge Measurement. In *Proceedings of the 1st International Group for Hydraulic Efficiency Measurement (IGHEM) Conference*, Montreal, Canada, June, 1996.

[6] A. Nichtawitz, P. Grafenberger, J. Tormann, and R. Gaisbauer. Discussion on Acoustic Flow Measurement Method. In *Proceedings of the 5th International Group for Hydraulic Efficiency Measurement (IGHEM) Conference*, Lucerne, Switzerland, July 14-16, 2004.

[7] K. Sugishita, A. Sakurai, H. Tanaka, and T. Suzuki. Evaluation error of acoustic method and its verification by comparative field tests. In *Proceedings of the 1st International Group for Hydraulic Efficiency Measurement (IGHEM) Conference*, Montreal, Canada, June, 1996.

[8] J. Lanzersdorfer. The use of the acoustic transit time method to determine the random uncertainty of planar velocity parameters in water. *Flow Measurement and Instrumentation*, 34:27–33, 2013.

[9] P. Lunde and K. E. Frøysa. *GERG Project on Ultrasonic Gas Flow Meters, Phase II.* VDI Verlag Düsseldorf, 2000.

[10] J. Hemp. Theory of transit time ultrasonic flowmeters. *Journal of Sound and Vibration*, 84(1):133–147, 1982.